Mutual Interdependence of the Physical Parameters Governing the Boundary-Layer Flow of Non-Newtonian Fluids

Samer Al-Ashhab [1,*] , **Dongming Wei** [2] , **Salem A. Alyami** [1] , **AKM Azad** [3,4] and **Mohammad Ali Moni** [5]

1 Department of Mathematics and Statistics, Faculty of Science, Imam Mohammad Ibn Saud Islamic University (IMSIU), Riyadh 13318, Saudi Arabia; saalyami@imamu.edu.sa
2 Department of Mathematics, Nazarbayev University, 53 Kabanbay Batyr Ave, Astana 010000, Kazakhstan; dongming.wei@nu.edu.kz
3 Faculty of Science, Engineering & Technology, Swinburne University of Technology, Sydney, NSW 2150, Australia; aazad@swin.edu.au
4 ProCan®, Children's Medical Research Institute, Faculty of Medicine and Health, The University of Sydney, Westmead, NSW 2145, Australia
5 Artificial Intelligence & Digital Health Data Science, School of Health and Rehabilitation Sciences, Faculty of Health and Behavioural Sciences, The University of Queensland, St Lucia, QLD 4072, Australia; m.moni@uq.edu.au
* Correspondence: ssashhab@imamu.edu.sa

Abstract: We consider non-Newtonian boundary-layer fluid flow, governed by a power-law Ostwald-de Waele rheology. Boundary-layer flows of non-Newtonian fluids have far-reaching applications, and are very frequently encountered in physical, as well as, engineering and industrial processes. A similarity transformation results in a BVP consisting of an ODE and some boundary conditions. Our aim is to derive highly accurate analytical relationships between the physical and mathematical parameters associated with the BVP and boundary-layer flow problem. Mathematical analyses are employed, where the results are verified at the numerical computational level, illustrating the accuracy of the derived relations. A set of "Crocco variables" is used to transform the problem, and, where appropriate, techniques are used to deal with the resulting singularities in order to establish an efficient computational setting. The resulting computational setting provides an alternative, which is different from those previously used in the literature. We employ it to carry out our numerical computations.

Keywords: boundary-layer flow; non-Newtonian fluid; power-law model; non-linear; singularity; semi-infinite domain; boundary-value problem

1. Introduction

Boundary-layer fluid-flow problems have been of much interest since their early development in the works of Schowalter and Acrivos et al. [1,2]. In [1] Schowalter derived the mathematical and physical formulations. However, the first numerical solutions were obtained by Acrivos et al. in [2]. The boundary-layer flow of non-Newtonian fluids assumes a variable viscosity. Classically the models are reduced by a similarity variable transformation from a system of coupled PDEs into a third-order non-linear ODE. The most commonly used model of the fluid is that of a power-law Ostwald-de Waele rheology, which is encountered quite often in the literature with many physical and industrial applications. We note that the power-law models are characterized by a power-law index n, where $n = 1$ corresponds to a Newtonian fluid. However, if $n > 1$ then the fluid is dilatant or shear-thickening, while the fluid is pseudo-plastic or shear-thinning if $0 < n < 1$. The reader is referred to [3–5] for further details on the general theory and applications of boundary layer non-Newtonian fluid flows.

Many variations of non-Newtonian boundary layer flows can be found in the literature with somewhat different governing equations and/or different sets of boundary conditions.

Numerical solutions can be found in many studies. For example, Denier and Dabrowski [6] found numerical solutions and used them to obtain a graphical representation for the relationship between the shear stress (also referred to as the wall shear or skin-friction coefficient) and a parameter *m* in the governing ODE. The parameter *m* was associated with a stream-wise velocity profile at infinity. They also discussed the difficulties associated with the numerical approaches employed to solve the ODE, and how to overcome them. Liao [7] also considered the difficulties involved in the numerical approaches and obtained numerical solutions for a different variant of the problem (consisting of a slightly different ODE). In [8], Chen et al. considered boundary layer flow of an electrically conducting non-Newtonian fluid in the presence of a magnetic field. They used the Adomian decomposition method (ADM) to obtain approximate solutions. They proceeded to find estimates for the value of the shear stress with relatively high accuracy. Zheng et al. [9] applied classical mathematical analysis to obtain bounds on the values of the shear stress, and compared their results to numerical estimates which showed the accuracy of their computations. Their upper and lower bounds showed a narrow range for large values of *n*.

Analytical solutions are also found in the literature. In [10], Guedda established an exact solution to a variant of the problem with certain boundary conditions that consist of a power-law velocity profile at infinity. He utilized symmetry methods to obtain his result. Bognár [11] obtained analytical solutions and proved existence and uniqueness using an approach involving the Briot–Bouquet Theorem. Wei and Al-Ashhab [12] established existence and uniqueness for all values of the power-law index *n* for a certain variant of the problem. Magyari et al. [13] also considered existence and uniqueness, where they determined parameter ranges for which solutions exist. They also determined parameter values where solutions do not exist. The interested reader is referred to the book by Merkin et al. [14] for a recent treatment of boundary-layer non-Newtonian fluid flow, with an extensive discussion of recent and novel applications (including applications of nanofluids, and micropolar fluids).

Similar solutions of power-law non-Newtonian fluid flow, not involving boundary layers, are also found in the literature. They exhibit very similar mathematical features to boundary-layer non-Newtonian flows. In this regard, Bedjaoui et al. [15] for example, established existence and uniqueness for a Rayleigh problem with Ostwald-de Wael electrically conducting fluids. Their study involved a second-order ODE. In [16], conditions for the existence and non-existence of self-similar solutions were determined for the two-dimensional Navier—Stokes equation involving non-Newtonian fluids.

Further applications of boundary-layer non-Newtonian fluids are found in the magnetohydrodynamics flow of fluids over a non-linear stretching sheet, cf. [17]. In these cases the problem was modeled by a coupled system of ODEs with the velocity, temperature and concentration as dependent variables. The authors needed to resort to numerical techniques and computers to solve the system of ODEs. Recent applications have involved micromixers with many applications in mechanical and chemical engineering. Researchers investigating microfluids and micromixers normally resort to numerical methods and algorithms to solve the corresponding coupled system of PDEs [18–20]. More applications of non-Newtonian fluid flow that became of interest in recent years can be found in the squeezing flow between two infinite plates [21–23]. Interesting applications that are considered involve a fourth-order non-linear ODE. All the recent applications constitute possible fields of application for our study and results. Applications of non-Newtonian fluids are far-reaching and it would not be possible to list all those who contributed in this field.

We intend to investigate the boundary-layer non-Newtonian fluid flow problem by applying analytical and computational approaches. Our aim is to use a "Crocco variable" transformation, which proved its efficiency in [24–26]. This technique was employed in [24] to investigate existence and uniqueness for Newtonian fluids which exhibited a *linear* model. It was employed in [25,26] to investigate existence and uniqueness, as well as properties of solutions for non-linear models. We shall investigate the same variant of the problem that was considered in [2,6,26] (with the same governing ODE and BCs). However, rather than obtaining numerical solutions, as in [2,6], and rather than investigating existence and

uniqueness of solutions, as in [26], we shall aim at finding relations between the different mathematical and physical parameters.

In Section 2, we introduce the problem, and determine how to deal with the resulting singularities in order to establish a reliable and efficient computational setting. This computational setting makes it possible to use computer integrators (computational methods) to obtain numerical measurements of the parameters. We derive our main results in Sections 3 and 4, where we employ classical mathematical analyses (and arguments). In Section 3, we derive a *mathematical* relationship between the cut-off values of the parameter m (where solutions do not exist past that point) and the power-law index n. This constitutes a very important and novel result, as, to the best of our knowledge, this has not been done before in any variant of the boundary-layer non-Newtonian fluid flow problem. One can only find numerical measurements of those parameters. In fact, the graphical relationships presented in [6] were based solely on numerical measurements of the parameters that were accomplished by computing machines. This would tell us what velocity profiles at infinity (of the form $u(x, \infty) = x^m$) are not possible to obtain, no matter what the wall shear ($f''(0)$) is. This is a natural result since it may not be physically possible for a profile with largely negative m to exist (in a domain reaching $x = 0$).

It turns out that the parameter m is crucial in the approximation and determination of the relationship between shear stress $f''(0)$ and m, as shall be illustrated in Section 4. The corresponding derived approximate relationship involves the power-law index n, so that it provides means to estimate $f''(0)$ for all values of n. The derived formulas constitute important new findings for several reasons. Firstly, we find out phenomena/methods to improve the accuracy of these formulas, yielding highly accurate estimates. Secondly, it is very likely that similar formulas will be obtained in other non-Newtonian fluid flow applications. Thirdly, the mathematical formulas may be used in future research, at the analytical level, to draw conclusions about the solutions, or reveal more properties of the parameters themselves.

2. Formulation

Boundary-layer flow of non-Newtonian fluids is classically modeled by the Cauchy equations, which constitute a coupled system of PDEs. Upon simplification, the 'scaled' Cauchy equations are obtained as follows:

$$\frac{\partial u}{\partial x} + \frac{\partial v}{\partial y} = 0 \tag{1}$$

$$u\frac{\partial u}{\partial x} + v\frac{\partial u}{\partial y} = u_e\frac{\mathrm{d}u_e}{\mathrm{d}x} + n\left|\frac{\partial^2 u}{\partial y^2}\right|^{(n-1)}\left(\frac{\partial^2 u}{\partial y^2}\right) \tag{2}$$

The reader is referred to [4,6] and the references therein for details of the derivation process as we aim to be brief and concise. The variables x and y represent the (scaled) spatial variables, while u and v represent the corresponding scaled orthogonal velocities of the moving fluid, in the x and y directions, respectively. A stream-wise velocity outside the boundary layer is assumed, where it is represented by $u_e(x)$ as in Equation (2). We shall assume $u_e(x) = x^m$ as was used in [6]. (We remark that in [10], the condition at infinity was given as $u = y^m$, see (3) below; however, the governing system of equations did not have the term involving u_e. Simpler boundary conditions at infinity are also found in the literature, cf. [1,25].) The boundary conditions of interest to us are (as in [2,6]):

$$u = v = 0 \text{ on } y = 0, \quad u \to u_e(x) \text{ as } y \to \infty \tag{3}$$

We remark that different sets of boundary conditions, in addition to the one above, are found in the literature. The Equations (1) and (2) admit self-similar solutions via the transformation:

$$u = x^m f'(\eta), \quad v = \alpha x^{s+m-1}\left(s\eta f'(\eta) - (s+m)f(\eta)\right) \tag{4}$$

where $s = (1 + m(n-2))/(n+1)$, $\alpha = n^{1/(n+1)}$, and where $\eta = y/(\alpha x^s)$ is a similarity variable. This reduces the system (1) and (2) into the following ODE:

$$\frac{1}{n}(|f''|^{n-1}f'')' = m((f')^2 - 1) - \frac{2mn - m + 1}{n + 1}ff'' \tag{5}$$

Remark 1. *The function f may be referred to as the shape function or the auto-similarity function.*

The boundary conditions (3) are transformed into:

$$f(0) = f'(0) = 0, \quad f'(\infty) = 1 \tag{6}$$

We shall assume positive curvature solutions where $f'' > 0$ on the entire solution domain. This is very typical in the literature and applications, c.f. [10,12,25]. Thus, we have the following boundary value problem:

$$(f'')^{n-1}f''' = m((f')^2 - 1) - kff'' \tag{7}$$

subject to

$$f(0) = 0, \quad f'(0) = 0, \quad f'(\infty) = 1, \tag{8}$$

where $k = \frac{2mn - m + 1}{n + 1}$.

Numerical solutions of this particular problem (7) and (8) can be found in [6]. Analytical investigation of this problem was conducted in [26], where the focus was mostly on existence and uniqueness in addition to the asymptotic behavior of solutions.

2.1. "Crocco Variables" and the Resulting Singularities

We introduce the following set of variables:

$$z = f'(\eta), \quad h(z) = (f''(\eta))^n. \tag{9}$$

These are similar to the classical Crocco variables which are given with new variables defined by $f(\eta)$ and $f'(\eta)$. The following transformed problem is obtained from (7)–(9)

$$h''(z) = \left(\alpha z - m(z^2 - 1)\frac{h'(z)}{h(z)}\right)h^{-1/n}(z), \quad 0 < z < 1, \tag{10}$$

subject to

$$h(1) = 0, \quad h(0) = (f''(0))^n, \quad h'(0) = -mn/f''(0), \tag{11}$$

and where

$$\alpha = 2mn - nk = \frac{(3m - 1)n}{n + 1}. \tag{12}$$

This transformation proves to be useful in the mathematical analysis of the original problem (7) and (8) and its parameters. It also provides an *alternative means* to obtain numerical results. This is in contrast to the technique that was used in [6], where the authors discuss the need for some careful treatments in determining the correct convergence for the boundary condition on the open end $(+\infty)$ for $n < 1$, whereas careful treatment was also needed when $n > 1$, as the solutions reach $f'' = 0$ identically at finite η (this observation was also proved at the analytical level for a similar problem in [12]). The advantage of using (10) and (11) in obtaining numerical solutions is that we deal with a finite domain and do not have to consider where or when to "stop". However, there is a problem that arises here and has to be addressed. The problem is dealing with the singularities of the equation. It is remarked that the singularity at the right end can be dealt with easily, since, as was illustrated in [26], solutions approach the point (1,0) linearly for $n > 1$. On the other hand, the solutions are integrable at $z = 1$ for $0 < n < 1$, despite the fact that gradients become infinite. In particular, the criterion for determining the values of m remains very simple as Runge–Kutta methods (used by Matlab) are effective at that end.

On the other hand, however, dealing with the singularity at $z = 0$ could lead to a serious problem on regular computing machines. This becomes more obvious when attempting to solve the ODE for $f''(0) = 0$, which is not mathematically possible in (11) above.

Remark 2. *Solving the ODE for $f''(0) = 0$ is crucial for us, as it corresponds to the cut-off values of m, as was observed in [6,26], and as is discussed in the introduction. The cut-off values of m are of much and particular interest in this fluid flow problem. We note that this is also a singularity of the original ODE (7).*

To circumvent this problem, it is necessary to take values of $f''(0)$ approaching (very close to) zero but the question arises of how small the values can be. Computing machines could then give erroneous and contradictory results when solving ODE (10) and seeking to determine the relevant parameter values that are of interest. These are typical and expected machine errors as smaller values of $f''(0)$ lead to extremely large derivatives, but also, and more importantly, they lead to extremely small values of $h(0)$, causing a problem that may be more serious for larger values of n (this may not occur due to the numerical method itself but rather due to a problem of the computing machines themselves). This problem, however, can be overcome as follows: Integrating Equation (10) from 0 to $z > 0$ leads to

$$h'(z) = -mn(1 - z^2)h^{-1/n} + \int_0^z (\alpha - 2mn)\mu h^{-1/n}(\mu)d\mu \qquad (13)$$

Observe that $h'(0) = -mn/f''(0)$ so that the initial conditions on both sides of the equation cancel out. Now, let $\epsilon(z) = \int_0^z (\alpha - 2mn)\mu h^{-1/n}(\mu)d\mu$ represent the error in the computation of $h'(z)$ in (13) above. We then have

$$h'(z) = -mn(1 - z^2)h^{-1/n} + \epsilon(z) \qquad (14)$$

Consider the case where $\alpha - 2mn < 0$ and let $-\delta > 0$ be the maximum of the absolute error $(-\epsilon(\mu))$ within the interval, which in this case happens to be at the right end, i.e., $\delta = \epsilon(z)$. It then follows that

$$\left(-(mn - \delta)z - \frac{mnz^3}{3}\right)^{\frac{n}{n+1}} < h(z) < \left(-mnz - \frac{mnz^3}{3}\right)^{\frac{n}{n+1}} \qquad (15)$$

Hence the error can be controlled. For example, an upper bound for the error due to the z^3 term can be determined by utilizing a classical Taylor-series approximation, and where the overall error obtained in $h'(z)$ is bounded by:

$$
\begin{aligned}
|\epsilon(z)| \quad < \quad & (\alpha - 2mn)(\delta - mn)^{-1/(n+1)} \int_0^z \mu^{n/(n+1)}d\mu \\
- \quad & \frac{mn}{3(n+1)}(\alpha - 2mn)(\delta - mn)^{-\frac{n-2}{n+1}} \int_0^z \mu^{(3n+2)/(n+1)}d\mu \\
\leq \quad & (\alpha - 2mn)(\delta - mn)^{-1/(n+1)} \frac{(n+1)}{(2n+1)}z^{(2n+1)/(n+1)} \\
- \quad & \frac{mn}{3(n+1)}(\alpha - 2mn)(\delta - mn)^{-\frac{n-2}{n+1}} \frac{(n+1)}{(4n+3)}z^{(4n+3)/(n+1)}.
\end{aligned}
$$

This is now required to be less than the desired error δ, which will give a value of z that can represent the starting point (away from the singularity) to solve the ODE with initial conditions $h(z), h'(z)$. It should be noted that when z is small enough the second term may be neglected. In all cases, however, the following can be used to find an initial estimate for z:

$$\left((\alpha - 2mn)(\delta - mn)^{-\frac{1}{(n+1)}} \cdot \frac{n+1}{2n+1}\right)z^{(2n+1)/(n+1)} = \delta \qquad (16)$$

Once z has been determined, the values of $h'(z)$ and $h(z)$ as well as the errors in measuring them, can be determined using (14) and (15) above. Note that both computations/approximations are overestimates. It should also be noted that the error in $h(z)$ remains much smaller than that in $h'(z)$, as can be seen by the equations above (and since h is an integration of h' taken here over a small interval).

3. Cut-Off Values for m

As discussed in the introduction, there is a cut-off value of m, say m_0, where solutions only exist for $m \geq m_0$, and do not exist for $m < m_0$. Determining the cut-off values m_0 analytically is a very interesting and important new result, which we shall obtain; the cut-off values m_0 can be determined analytically. This was performed numerically in [6] for certain values of n over a limited range. We shall obtain numerical computations for m_0 over a wide range of n, and also derive a mathematical formula that provides the values of m_0 (in terms of n) with relatively high accuracy.

It is remarked here that the graphs in [6] may suggest that for $n > 1$ there may be a minimum value of $|m_0|$ for all n, with some focal point at some $m > m_0$ where all graphs intersect. In fact, this can be shown to be false by contradiction. Suppose it were true, then there would be some $m_0 = M < 0$ where solutions exist for all n, but then, from (15), we would have h as an increasing function on (0,1) for large n. This, in turn, implies that a solution where $h(1) = 0$ could not exist, constituting a contradiction. This shows that $m_0 \to 0$ as $n \to \infty$. In fact, assuming $m_0 < -\frac{\kappa}{n^p} (\kappa > 0)$ for large n leads to a contradiction, similar to the one above, whenever $p < 1$.

On the other hand, assume $m_0 < -\frac{\kappa}{n}$. This would imply that the solution gradient is $h'(z_0) \approx \kappa$ at some very small $z_0 > 0$. At the same time, we would have $h(z_0) \approx 0$. In fact, at the point where $z = \sqrt{-m}$, the two terms in the governing Equation (10) become comparable and almost equal for m very close to zero. Therefore, if we take z_0 proportional to $\sqrt{-m}$, or say $z_0 = (-m)^p$ for some $p > 1/2$ but close to $1/2$, then the second term in (10) becomes negligible with m very close to zero and large n. We can then use the estimate $h'(z) \approx \kappa + \alpha z^2/2$ on $(z_0, 1)$ leading to $h(1) \approx \kappa + \alpha/6$. In particular, if $\kappa > 1/6$ then it must be that $h(1) > 0$, so that $h(1) = 0$ could not be satisfied and a solution would not exist. (A mathematically precise classical ϵ-δ argument can be made here, but we choose to omit it and focus on what is more relevant to us from the practical viewpoint). We have shown that

Proposition 1. *A solution to (7) and (8) does not exist whenever*

$$m < m_0 = -\frac{1}{6n + c} \tag{17}$$

where $c = c(n)$ is of an order less than one in n.

Remark 3. *The result that we have established here for the value of m_0 (for large n), as in (17), exhibits a* significant *improvement from what has been observed in [26] where it was shown that a solution does not exist for $m < -\frac{1}{2n+1}$.*

In fact, it was found numerically that c could be approximated to a constant where the cut-off value of m would be given as $m_0 \approx -\frac{1}{6n+c}$. Table 1 shows some numerical values of m_0 and the corresponding values of c for different values of n, spanning over a relatively wide range. Observe that the sequence of values of c in the table suggests a convergence to occur, for large n, to a value around 4.33 (or some value likely greater than 4, or possibly greater than 4.3).

This is a very useful result at the practical level. At the same time, it is a very peculiar mathematical observation that requires further analytical study at the mathematical level. From a practical point of view, if one uses (17) with $c = 4.35$ as an approximation for m_0 over the wide range $50 < n < 500$, then the relative error in the corresponding estimates of

m_0 would be less than 0.002%, providing accuracy up to the fifth non-zero decimal place (or better) in most readings. Similarly, a suitable value of c can be chosen to provide the desired accuracy for different ranges of n. The span of those ranges, however, may have to be relatively small for smaller values of n (and if the required accuracy is relatively high).

Table 1. Smallest value of m where a solution for (7) and (8) exists .

n	5	15	30	50
m_0	-0.0289496	-0.010591	-0.0054235	-0.0032856
c	4.55	4.42	4.38	4.36
n	100	150	200	500
m_0	-0.00165466	-0.00110577	-0.000830331	-0.000332853
c	4.35	4.35	4.34	4.33

4. Estimating Shear Stress Versus m

We seek to derive an analytical (mathematical) relationship between $f''(0)$ and m. To that end, recall the approximations in (14) and (15) around $z = 0$. In particular, observe that, if $h(0) = (f''(0))^n \neq 0$, we then have

$$h(z) \approx ((h(0))^{\frac{n+1}{n}} - mnz)^{\frac{n}{n+1}} = ((f''(0))^{(n+1)} - mnz)^{\frac{n}{n+1}}. \tag{18}$$

Now, to determine a relationship between m and $f''(0)$ close to the point $(m_0, 0)$, consider the rate of change of $f''(0)$ with respect to m at $m = m_0$ (note that $f''(0) = 0$ at this cut-off value of m). We must consider a small change in m, say Δm. To this end, fix some z close to 0; we seek that $h(z)$ (at that point) does not change as m changes, for the following explanation. First, note that this shall require that Δm be proportional to $(f''(0))^{n+1}$. Observe that this will then imply that the corresponding changes in $h(z)$ and $h'(z)$ are, mathematically, of orders higher than 1 in Δm. It is not difficult to see that, past this point, the change (variation) in h over the solution interval $(z, 1)$ should remain within orders higher than 1 in Δm (see Equation (10)). Thus, the overall change in h over the interval $(z, 1)$ will be of higher orders of Δm. Consequently, we must have $h(1) = 0$ satisfying the boundary condition at the right end. We point out that the mathematical details can be worked out with the techniques of the calculus of variations. However the details are of an abstract mathematical nature, and would not be of direct relevance to our main conclusions and results, so we choose to omit them.

The above discussion and mathematical arguments provide the approximate relationship for $f''(0)$ versus m (for m close to m_0) up to orders of Δm greater than 1:

$$f''(0) \approx \beta(m - m_0)^\gamma, \quad \gamma \approx \frac{1}{n+1} \tag{19}$$

Remark 4. *Observe that the above approximation provides an exact relationship for infinitesimal changes in the parameters. Additionally, note that h' remains finite for z close to $z = 1$ for $n > 1$, while it remains integrable around $z = 1$ for $n < 1$, as discussed earlier (see [26]). This shows that the provided approximation is anticipated to be better for larger values of n (but should stay valid for all n).*

4.1. Comparison with Computed Values

We compare the shear stress ($f''(0)$) estimates obtained via the derived approximation (19) with computed values obtained via computing machines (Matlab). Each of the following tables include two "sample points" that are used to determine the values of β and γ in (19) above. Tables 2 and 3 are for dilatant fluids ($n > 1$), while Tables 4 and 5 are for pseudo-plastic fluids ($n < 1$).

Table 2. Computed and estimated values for shear stress versus m for $n = 5$. The points where $f''(0) = 0.2$ and $f''(0) = 0.25$ are taken as sample points in determining the approximation.

m	-0.0289356	-0.0288963	-0.0287912	-0.0280749	-0.0256965
$f''(0)$	0.2	0.25	0.3	0.4	0.5
$f''(0)$ (est.)	$-$	$-$	0.300	0.399	0.497
relative error	$-$	$-$	0.06%	0.25%	0.6%

Table 3. Computed and estimated values for shear stress versus m for $n = 1.5$. The points where $f''(0) = 0.1$ and $f''(0) = 0.15$ are taken as sample points in determining the approximation.

m	-0.069598	-0.065791	-0.059837	-0.051543	-0.040742
$f''(0)$	0.1	0.15	0.2	0.25	0.3
$f''(0)$ (est.)	$-$	$-$	0.1985	0.2461	0.2931
relative error (est.)	$-$	$-$	0.75%	1.56%	2.3%
$f''(0)$ (improved)	$-$	$-$	0.20004	0.24998	0.29981
relative error (impr.)	$-$	$-$	0.02%	0.008%	0.063%
m	-0.027251	-0.010885	0	0.02	0.04
$f''(0)$	0.35	0.4	0.429002	0.476168	0.51756
$f''(0)$ (est.)	0.33969	0.38607	0.41333	0.45661	0.49496
relative error (est.)	2.95%	3.48%	3.65%	4.11%	4.37%
$f''(0)$ (improved)	0.34969	0.39972	0.42883	0.47639	0.51834
relative error (impr.)	0.086%	0.075%	0.04%	0.047%	0.15%

Table 4. Computed and estimated values for shear stress versus m for $n = 0.8$. The points where $m = -0.09$ and $m = -0.085$ are taken as sample points in determining the approximation.

m	-0.09	-0.085	-0.08	-0.075	0
$f''(0)$	0.070869	0.090022	0.10699	0.12219	0.28582
$f''(0)$ (est.)	-	-	0.10647	0.12119	0.26861
relative error (est.)	-	-	0.49%	0.82%	6.0%
$f''(0)$ (improved)	-	-	0.106954	0.12239	0.28638
relative error (impr.)	-	-	0.034%	0.164%	0.196%

Table 5. Computed and estimated values for shear stress versus "large" values of m for $n = 0.8$. The points where $m = 1.8$ and $m = 1.9$ are taken as sample points in determining the approximation.

m	1.5	1.8	1.9	2	2.1	2.2
$f''(0)$	1.4550	1.6033	1.6503	1.6963	1.7413	1.78541
$f''(0)$ (est.)	1.4554	-	-	1.6963	1.7413	1.78547
relative error	0.027%	-	-	0.0008%	0.0017%	0.0034%

Table 2 illustrates the relatively accurate relationship (19) in estimating the values of shear stress versus m for $n = 5$, and where the first two points are used as the "sample points" to determine β and γ.

Remark 5. *We note the existence of an interesting and very useful feature here: if the formula is adjusted/determined using two "sample points" far from the vertex to yield a new β and γ, then its accuracy can be highly improved in that neighbourhood. For example, it is found out that $f''(0) = 0.726$ for $m = 0$, but the estimated value from the formula is $f''(0) = 0.715$. However, when using the points where $f''(0) = 0.4$ and $f''(0) = 0.5$ as sample points, then the adjusted formula yields an estimate of $f''(0) = 0.7249$. This shows a highly significant improvement in accuracy by ten-fold.*

As for Table 3 where $n = 1.5$, note that we have $m_0 = -0.0718478$. The estimated values for $f''(0)$ using (19) are shown in the table, where β and γ are determined using the two points where $f''(0) = 0.1$ and $f''(0) = 0.15$ as sample points. Once again, a relatively good accuracy is illustrated using the root formula (19).

Additionally, note that, as before, if we choose different sample points, then higher accuracy is obtained within their corresponding neighbourhood. In particular, when using the points where $m = 0$ and $m = 0.02$ to obtain the root formula, we find that the estimate for the shear stress $f''(0)$ at the point where $f''(0) = 0.4$ (to the left) is 0.4001, while the estimate for $f''(0)$ at $m = 0.04$ (on the right) is 0.51772. Taking a "farther" point, such as the one where $m = 0.2$ (not shown in Table 3), we have $f''(0) = 0.75028$ while the estimated value is 0.75496. However, taking the points where $m = 0.16$ and $m = 0.18$ (not shown in the table), as sample points to determine the corresponding root formula, one obtains an estimated value of $f''(0) = 0.75032$ at $m = 0.2$. This shows a highly significant improvement (for a relatively large spacing of 0.02 in m).
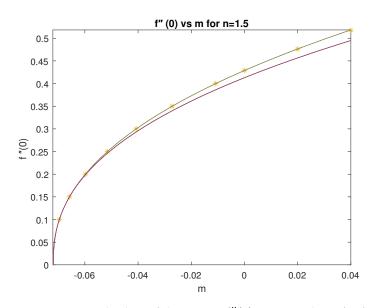
Table 4 shows the comparison between the computed and estimated values of shear stress where $n = 0.8$, for points close to the vertex of the root at $m_0 = -0.09956$. Table 5, however, shows the comparison for $n = 0.8$ for points that are farther away from the vertex. Observe that the sample points are changed. Note also that even though the spacing is larger, the approximation is (naturally) better since the points are farther away from the vertex.

Remark 6. *Observe that the computed values for γ up to four decimal places are $\gamma = 0.1669 \approx 1/6$ for $n = 5$, $\gamma = 0.4094 \approx 1/2.5$ for $n = 1.5$, and $\gamma = 0.5686 \approx 1/1.8$ for $n = 0.8$. This is consistent with the above approximation (19) where $\gamma \approx \frac{1}{n+1}$. The deviation is explained by the fact that the sample points for the measurement are not within infinitesimal distances from m_0. Note also that these approximations are better for larger values of n.*
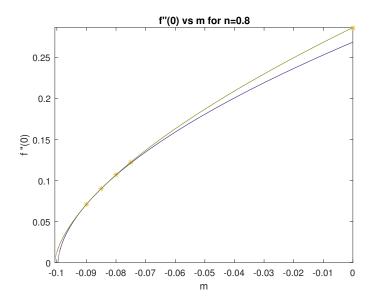
4.2. Improving the Approximation

A rather *interesting phenomenon* has been observed. If the "vertex" of the root graph/formula (19) is shifted using a different value for m_0, then *highly improved* estimates are obtained for $f''(0)$. For example, if we shift the "vertex" for $n = 1.5$, so that we assume $m_0 = -0.072019$ (instead of -0.0718478), then highly improved estimates for $f''(0)$ are obtained. This is illustrated in Table 3 and Figure 1. We remark that the sample points remain unchanged. Similarly, for $n = 0.8$, the vertex can be shifted to obtain a highly improved approximation. Table 4 shows the highly improved estimates that are obtained when using $m_0 = -0.10066$ for the vertex (instead of $m_0 = -0.09956$). This is also illustrated in Figure 2.

This is a very peculiar and extremely useful phenomenon, as it drastically improves the accuracy. It would be interesting and very beneficial to study this phenomenon more thoroughly at the mathematical level in future research in the field. Even though the current "ad hoc" trial-and-error approach in determining the new vertex is not tedious, especially given the highly improved results, it would be very worthwhile to explore the possibility of a mathematical formula that could determine the vertex shift in a more exact fashion.

Figure 1. Computed values of shear stress $f''(0)$ at some values of m for a dilatant fluid ($n = 1.5$): "*".
Estimated values using (19): Purple. Improved values by adjusting m_0 in (19): Green. (See Table 3).

Figure 2. Computed values of shear stress $f''(0)$ at some values of m for a pseudo-plastic fluid
($n = 0.8$): "*". Estimated values using (19): Purple. Improved values by adjusting m_0 in (19): Green.
(See Table 4).

5. Conclusions

We have considered the boundary-layer flow of non-Newtonian fluids that are modeled by an Ostwald-de Waele power-law rheology. A "Crocco variable" transformation was applied where the resulting singularities were dealt with numerically, so as to establish an efficient means to obtain accurate solutions and compute the relevant parameters. This also helped to efficiently avoid computing machine errors at/around the singularities. Mathematical techniques and analyses were applied to establish highly accurate explicit relationships between the physical and mathematical parameters. In particular, a mathematical relationship was explicitly determined between the power-law index n and the cut-off values of m where solutions cease to exist. A relationship between the shear stress $f''(0)$ and m was also derived.

The numerical computations provided insight into the peculiar details and "properties" of the derived relations. In particular, it was found that modifications and adjustments

of those relationships could lead to a highly improved accuracy. This improved accuracy was observed both locally when working in a certain range of the parameters, as well as for wider ranges. The improvements were very significant and therefore warrant further study, exploration, and research, both at mathematical and practical levels. The obtained results were also significant from the viewpoint that previous studies, such as [6], showed the interdependence of the parameters only at a numerical graphical level, and only for limited ranges of the parameters. It should also be noted that our results hold for both dilatant ($n > 1$), as well as, pseudo-plastic fluids ($n < 1$).

Author Contributions: Conceptualization, S.A.-A. and D.W.; Data curation, M.A.M.; Formal analysis, S.A.-A., D.W., S.A.A., A.A. and M.A.M.; Funding acquisition, S.A.-A. and S.A.A.; Investigation, S.A.-A., D.W., S.A.A. and A.A.; Methodology, S.A.-A. and D.W.; Project administration, D.W.; Resources, D.W., S.A.A., A.A. and M.A.M.; Software, S.A.-A., S.A.A., A.A. and M.A.M.; Supervision, D.W.; Validation, D.W. and M.A.M.; Visualization, M.A.M.; Writing—original draft, S.A.-A. and D.W.; Writing—review & editing, S.A.-A., D.W., S.A.A., A.A. and M.A.M. All authors have read and agreed to the published version of the manuscript.

Conflicts of Interest: The authors declare no conflict of interest. The funders had no role in the design of the study; in the collection, analyses, or interpretation of data; in the writing of the manuscript, or in the decision to publish the results.

References

1. Schowalter, W.R. The application of boundary-layer theory to power-law pseudoplastic fluids: similar solutions. *Aiche J.* **1960** *6*, 24–28. [CrossRef]
2. Acrivos, A.; Shah, M.J.; Petersen, E.E. Momentum and heat transfer in laminar boundary-layer flow of non-Newtonian fluids past external surfaces. *Aiche J.* **1960** *6*, 312–317. [CrossRef]
3. Astarita, G.; Marrucci, G. *Principles of Non–Newtonian Fluid Mechanics*; McGraw-Hill: New York, NY, USA, 1974.
4. Bird, R.B.; Armstrong, R.C.; Hassager, O. *Dynamics of Polymeric Liquids*; Wiley: Hoboken, NJ, USA, 1977.
5. Schlichting, H. *Boundary Layer Theory*; McGraw-Hill Press: New York, NY, USA, 1979.
6. Denier, J.P.; Dabrowski, P. On the boundary-layer equations for power-law fluids. *Proc. R. Soc. Lond.* **2004**, *460*, 3143–3158. [CrossRef]
7. Liao, S.J. A challenging nonlinear problem for numerical techniques. *J. Comput. Appl. Math.* **2005**, *181*, 467–472. [CrossRef]
8. Chen, X.; Zheng, L.; Zhang, X. MHD boundary layer flow of a non-Newtonian fluid on a moving surface with a power-law velocity. *Chin. Phys. Lett.* **2007**, *24*, 1989–1991.
9. Zheng, L.; Zhang, X.; He, J. Existence and estimate of positive solutions to a nonlinear singular boundary value problem in the theory of dilatant non-Newtonian fluids. *Math. Comput. Model.* **2007**, *45*, 387–393. [CrossRef]
10. Guedda, M. Boundary-layer equations for a power-law shear driven flow over a plane surface of non-Newtonian fluids. *Acta Mech.* **2009**, *202*, 205–211. [CrossRef]
11. Bognár, G. Similarity solution of a boundary layer flow for non-Newtonian fluids. *Int. J. Nonlinear Sci. Numer. Simul.* **2010**, *10*, 1555–1566. [CrossRef]
12. Wei, D.; Al-Ashhab, S. Similarity Solutions for a non-Newtonian power-law fluid flow. *Appl. Math. Mech.* **2014**, *35*, 1155–1166. [CrossRef]
13. Magyari, E.; Keller, B.; Pop, I. Boundary-layer similarity flows driven by a power-law shear over a permeable plane surface. *Acta Mech.* **2003**, *163*, 139–146. [CrossRef]
14. Merkin, J.H.; Pop, I.; Lok, Y.; Grosan, T. *Similarity Solutions for the Boundary Layer Flow and Heat Transfer of Viscous Fluids, Nanofluids, Porous Media, and Micropolar Fluids*; Academic Press: Cambridge, MA, USA, 2021.
15. Bedjaoui, N.; Guedda, M.; Hammouch, Z. Similarity Solutions of the Rayleigh problem for Ostwald-de Wael electrically conducting fluids. *Anal. Appl.* **2011**, *9*, 135–159. [CrossRef]
16. Wei, D.; Al-Ashhab, S. Existence of self-similar solutions of the two-dimensional Navier–Stokes equation for non-Newtonian fluids. *Arab. J. Math. Sci.* **2019** , *26*, 167–178. [CrossRef]
17. Wahab, H.A.; Zeb, H.; Bhatti, S.; Gulistan, M.; Kadry, S.; Nam, Y. Numerical Study for the Effects of Temperature Dependent Viscosity Flow of Non-Newtonian Fluid with Double Stratification. *Appl. Sci.* **2020**, *10*, 708. [CrossRef]
18. Kouadri, A.; Douroum, E.; Lasbet, Y.; Naas, T.; Khelladi, S.; Makhlouf, M. Comparative study of mixing behaviors using non-Newtonian fluid flows in passive micromixers. *Int. J. Mech. Sci.* **2021**, *201*, 106472. [CrossRef]
19. Galletti, C.; Mariotti, A.; Siconolfi, L.; Mauri, R.; Brunazzi, E. Numerical investigation of flow regimes in T-shaped micromixers: Benchmark between finite volume and spectral element methods. *Can. J. Chem. Eng.* **2019** *97*, 528–541. [CrossRef]

20. Jegatheeswaran, S.; Ein-Mozaffari, F.; Wu, J. Laminar mixing of non-Newtonian fluids in static mixers: process intensification perspective. *Rev. Chem. Eng.* **2020** *36*, 423–436. [CrossRef]
21. Ran, X.J.; Zhu, Q.Y.; Li, Y. An explicit series solution of the squeezing flow between two infinite plates by means of the homotopy analysis method. Commun. *Nonlinear Sci. Numer. Simul.* **2009** *14*, 119–132. [CrossRef]
22. Filobello-Nino, U.; Vazquez-Leal, H.; Cervantes-Perez, J.; Benhammouda, B.; Perez-Sesma, A.; Hernandez-Martinez, L.; Jimenez-Fernandez, V.M.; Herrera-May, A.L.; Pereyra-Diaz, D.; et al. A Handy Approximate Solution for a Squeezing Flow between Two Infinite Plates by Using of Laplace Transform-Homotopy Perturbation Method. *SpringerPlus* **2014**, *3*, 421. [CrossRef]
23. Shamshuddin, Md.; Mishra, S.R.; Anwar Beg, O.; Kadir, A. Viscous Dissipation and Joule Heating Effects in Non-Fourier MHD squeezing flow. *Arab. J. Sci. Eng.* **2019**, *44*, 8053–8066. [CrossRef]
24. Nachman, A.; Taliaferro, S. Mass transfer into boundary-layers for power-law fluids. *Proc. R. Soc. Lond.* **1979**, *365*, 313–326.
25. Al-Ashhab, S. Asymptotic Behavior and Existence of Similarity Solutions for a Boundary Layer Flow Problem. *Kuwait J. Sci.* **2019**, *46*, 13–20.
26. Al-Ashhab, S. Properties of boundary-layer flow solutions for non-Newtonian fluids with non-linear terms of first and second-order derivatives. *J. Eng. Math.* **2020**, *123*, 29–39. [CrossRef]